

Engineering Double to Quintuple Stacks of a Polarized Aromatic in Confined Cavities

Yoshihiro Yamauchi,[†] Michito Yoshizawa,^{*,‡,§} Munetaka Akita,[‡] and Makoto Fujita^{*,†}

Department of Applied Chemistry, School of Engineering, The University of Tokyo, 7-3-1 Hongo, Bunkyo-ku, Tokyo 113-8656, Japan, and Chemical Resources Laboratory, Tokyo Institute of Technology, and PRESTO (JST), 4259 Nagatsuta, Midori-ku, Yokohama 226-8503, Japan

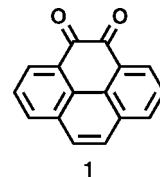
Received May 19, 2009; E-mail: yoshizawa.m.ac@m.titech.ac.jp; mfujita@appchem.t.u-tokyo.ac.jp

Abstract: Discrete, well-defined stacks of the polarized aromatic pyrene-4,5-dione (**1**) were assembled in the cavities of organic-pillared coordination cages (**2**). The number (n) of stacked guests depends on the pillar length, and up to quintuple stacks ($n = 5$) were observed when long (16.5 Å) organic pillar ligands were incorporated. As previously reported, pyrene-4,5-dione (**1**) assembles into infinite columnar stacks in the solid state, but the present work demonstrates that the polarized **1** has a strong propensity to stack in layers even in the absence of crystal packing effects. For $n = 2$ and 3 structures, crystallographic studies revealed that **1** stacks by π - π interactions in the cavity in such a way that a net dipole moment is canceled. These results emphasize the important role of dipole-dipole interactions as well as π -stacking interactions in the formation of columnar stacks of **1**.

Introduction

Dipole-dipole interactions between polarized molecules are important but relatively weak attractive forces that can control molecular orientations in supramolecular assemblies and arrays.¹ In the solid state, polar molecules typically pack in such a way that the net dipole is canceled. By utilizing the dipole-dipole interaction, Müllen et al. engineered infinite columnar stacks of polarized aromatic compounds in the crystalline state.² Their principal aromatic, pyrene-4,5-dione (**1**),³ stacks in an offset head-to-tail fashion due to the large dipole moment, 6.1–6.7 D. The question then arises whether the alternating stacked array is induced predominantly by dipole-dipole interactions or by crystal packing effects. To eliminate the latter and evaluate the role of dipole-dipole interactions in the stacking of **1**, a method to assemble stacks in the absence of crystal packing is required.

As a tool for studying discrete aromatic stacks in solution,⁴ we have recently developed organic-pillared coordination cages of the general formula of **2** (Figure 1).⁵ Within the constrictive



cavity⁶ of the self-assembled box-shaped coordination cages **2a–2f**, planar molecules assemble into discrete stacks. The number of planar guest molecules depends on the cavity height, which is determined by the pillar length. Cages **2a–2f** were designed to accommodate one to five planar guest molecules in the cavities. Previous studies have shown that large electron rich donor aromatics (e.g., pyrene, perylene, and coronene) efficiently form single and double stacks (i.e., **2a**⊂(G) and **2b**⊂(G)₂) with the electron poor panels of host **2** by π -stacking

[†] The University of Tokyo.

[‡] Tokyo Institute of Technology.

[§] PRESTO (JST).

- (1) (a) Kishikawa, K.; Harris, M. C.; Swager, T. M. *Chem. Mater.* **1999**, *11*, 867–871. (b) Levitsky, I. A.; Kishikawa, K.; Eichhorn, S. H.; Swager, T. M. *J. Am. Chem. Soc.* **2000**, *122*, 2474–2479. (c) Kishikawa, K.; Furusawa, S.; Yamaki, T.; Kohmoto, S.; Yamamoto, M.; Yamaguchi, K. *J. Am. Chem. Soc.* **2002**, *124*, 1597–1605. (d) Bushby, R. J.; Boden, N.; Kilner, C. A.; Lozman, O. R.; Lu, Z.; Liu, Q.; Thornton-Pett, M. A. *J. Mater. Chem.* **2003**, *13*, 470–474. (e) Jiang, J.; Lima, O. V.; Pei, Y.; Zeng, X. C.; Tan, L.; Forsythe, E. *J. Am. Chem. Soc.* **2009**, *131*, 900–901.
- (2) Wang, Z.; Enkelmann, V.; Negri, F.; Müllen, K. *Angew. Chem., Int. Ed.* **2004**, *43*, 1972–1975.
- (3) (a) Vollmann, H.; Becker, H.; Corell, M.; Streeck, H.; Langbein, G. *Justus Liebig's Ann. Chem.* **1937**, *531*, 1–159. (b) Young, E. R. R.; Funk, R. L. *J. Org. Chem.* **1998**, *63*, 9995–9996. (c) Hu, J.; Zhang, D.; Harris, F. W. *J. Org. Chem.* **2005**, *70*, 707–708.

- (4) (a) Misumi, S. *Cyclophanes*; Keehn, P. M., Rosenfeld, S., Eds.; Academic Press: New York, 1983; pp 573–628. (b) Hill, D. J.; Mio, M. J.; Prince, R. B.; Hughes, T. S.; Moore, J. S. *Chem. Rev.* **2001**, *101*, 3893–4011. (c) Klosterman, J. K.; Yamauchi, Y.; Fujita, M. *Chem. Soc. Rev.* **2009**, *38*, 1714–1725.
- (5) (a) Kumazawa, K.; Biradha, K.; Kusakawa, T.; Okano, T.; Fujita, M. *Angew. Chem., Int. Ed.* **2003**, *42*, 3909–3913. (b) Yoshizawa, M.; Nakagawa, J.; Kumazawa, K.; Nagao, M.; Kawano, M.; Ozeki, T.; Fujita, M. *Angew. Chem., Int. Ed.* **2005**, *44*, 1810–1813.
- (6) (a) Leininger, S.; Olenyuk, B.; Stang, P. J. *Chem. Rev.* **2000**, *100*, 853–908. (b) Steed, J. W.; Atwood, J. L. *Supramolecular Chemistry*; John Wiley & Sons, Ltd.: England, 2000. (c) Warmuth, R.; Yoon, J. *Acc. Chem. Res.* **2001**, *34*, 95–105. (d) Hof, F.; Craig, S. L.; Nuckolls, C.; Rebek, J., Jr. *Angew. Chem., Int. Ed.* **2002**, *41*, 1488–1508. (e) Fiedler, D.; Leung, D. H.; Bergman, R. G.; Raymond, K. N. *Acc. Chem. Res.* **2005**, *38*, 349–358. (f) Fujita, M.; Tominaga, M.; Hori, A.; Therrien, B. *Acc. Chem. Res.* **2005**, *38*, 371–380. (g) Vriezema, D. M.; Aragones, M. C.; Elemans, J. A. A. W.; Cornelissen, J. J. L. M.; Rowan, A. E.; Nolte, R. J. M. *Chem. Rev.* **2005**, *105*, 1445–1490. (h) Amijs, C. H. M.; van Klink, G. P. M.; van Koten, G. *Dalton Trans.* **2005**, 308–327. (i) Yoshizawa, M.; Klosterman, J. K.; Fujita, M. *Angew. Chem., Int. Ed.* **2009**, *48*, 3418–3438.

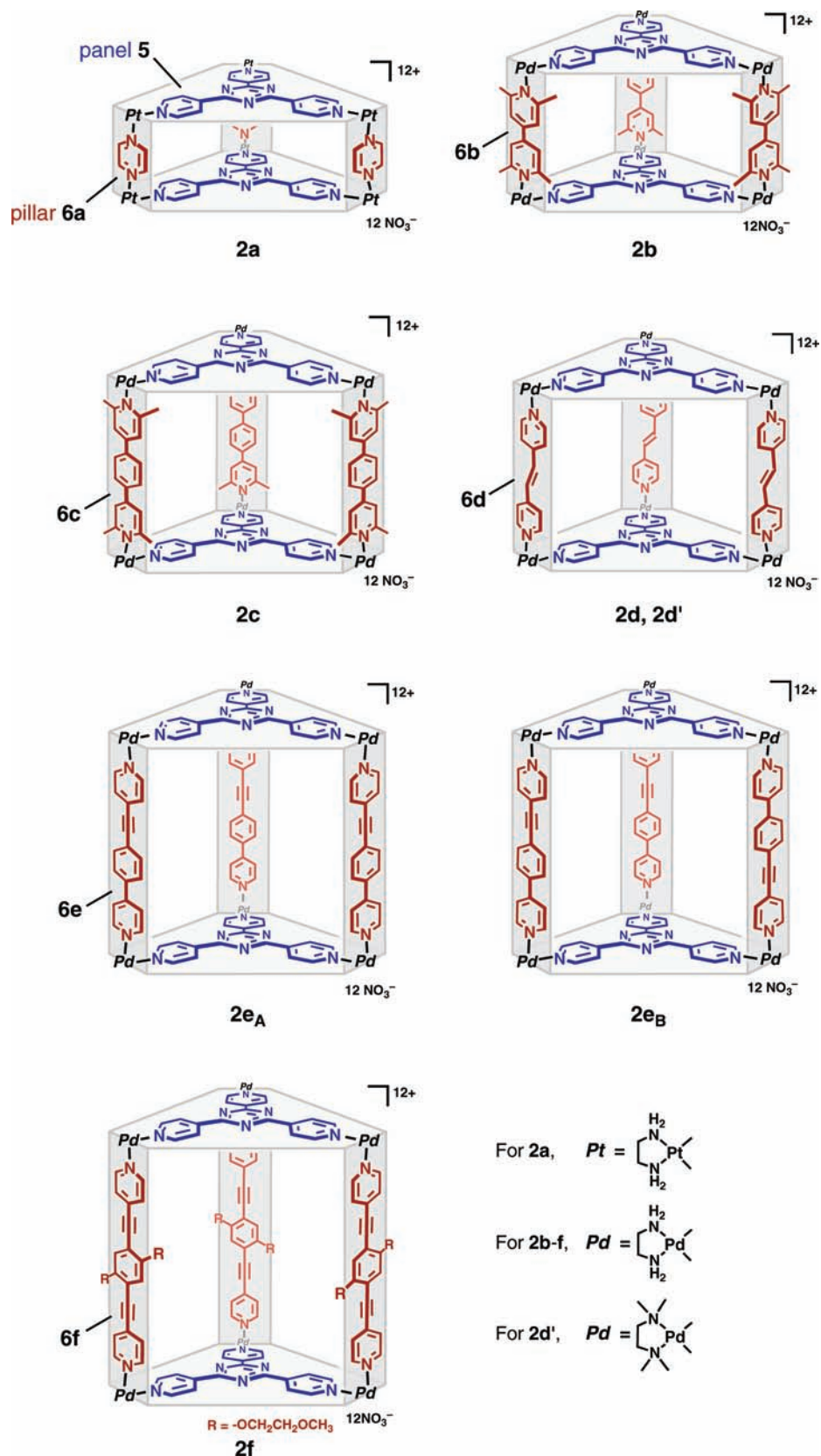


Figure 1. Chemical structures of organic-pillared coordination cages (2a–2f), panel ligand (5), pillar ligand (6a–6f), and metal hinge (7).

interactions but triple DDD stacks are disfavored due to the electrostatic repulsions.⁵ Assuming that otherwise weak dipole–dipole interactions help multiple π -stacks of large aromatic

guests, we examined the stacking of polarized large aromatic molecule **1** in the cavities of pillared cages **2a–2f**.⁷ The present study revealed that not only π -stacking interactions but also

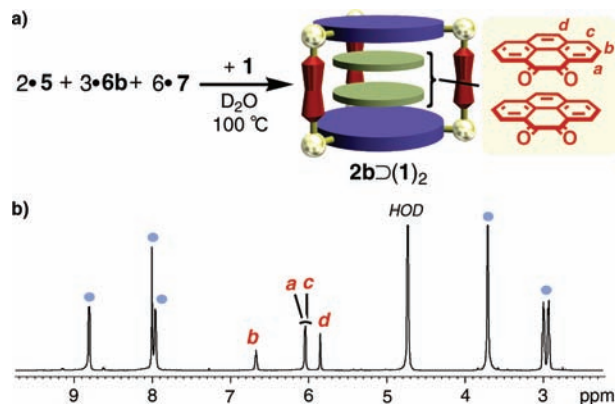


Figure 2. (a) Schematic representation of the self-assembly of double stack $2b\supset(1)_2$ complex and (b) the ^1H NMR spectrum (500 MHz, 300 K) in D_2O (light blue circle: cage $2b$).

dipole–dipole interactions and not crystal packing are responsible for the assembly and orientation of stable discrete stacked structures $(1)_n$ ($n = 2$ –5) in the cavities of 2 .

Results and Discussion

Double Stack ($2b\supset(1)_2$). 4,4'-Bipyridine pillar ligand $6b$ is the ideal height to generate a pillared cage with a space ideally sized for dimer $(1)_2$. The methyl substituents on ligand $6b$ are necessary as their steric bulk prevents formation of the homotopic M_6L_4 cage⁸ and $M_4L'_4$ square complexes.⁹ Pyrene-4,5-dione (1), pillar $6b$, triazine ligand 5 , and (en) $\text{Pd}(\text{NO}_3)_2$ (7) were combined in a 2.2:3:2:6 ratio in water and stirred at 100 °C. After 3 h, the pale-yellow heterogeneous solution turned a clear deep orange. Formation of complex $2b\supset(1)_2$ was evidenced by 1D and 2D NMR analyses (Figure 2). After inclusion, the ^1H NMR signals of guest 1 are shifted considerably upfield ($\Delta\delta = -1.11 \sim -2.47$ ppm) due to shielding by the aromatic panels of $2b$. The 2D DOSY spectrum supports a single host–guest structure with a single diffusion coefficient ($D = 1.5 \times 10^{-10} \text{ m}^2 \text{ s}^{-1}$).¹⁰

The $2b\supset(1)_2$ structure was unambiguously determined by single-crystal X-ray analysis. Deep-orange crystals were obtained from the aqueous solution of $2b\supset(1)_2$ by the slow evaporation of water and subjected to diffraction study. The crystal structure revealed that two molecules of 1 are stacked to each other with 3.3 Å interplanar distances within cage $2b$ (Figure 3). The dimer $(1)_2$ is disordered and located at three positions (Figure S32, Supporting Information). However, at each position exists a pair of 1 stacked in an alternating, head-to-tail fashion. The head-to-tail pair closely resembles the crystal structure that obtained from 1 itself² and the alternating stacking manner cancels the local, and net, dipole moment. Although

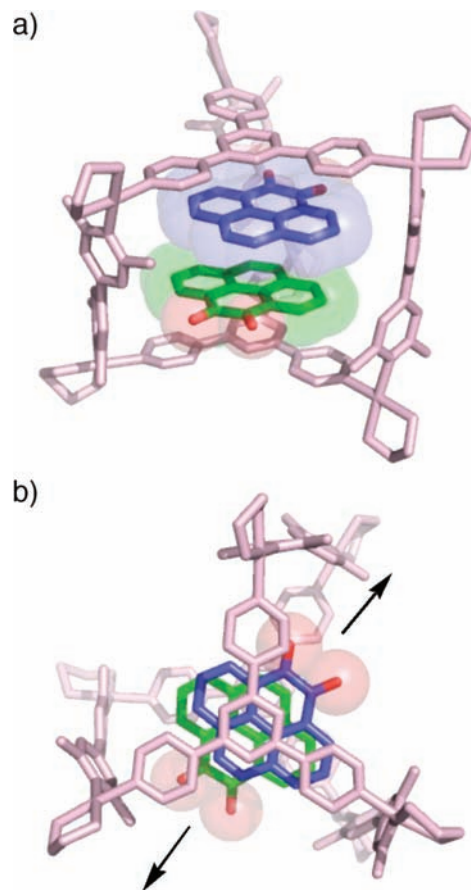


Figure 3. X-ray crystal structure of $2b\supset(1)_2$. The dimer $(1)_2$ is disordered at three positions. Only the dimer with the highest occupancy is shown. Hydrogen atoms, solvent molecules (H_2O) and counteranions (NO_3^-) are omitted for clarity. (a) Side view and (b) top view; Carbonyl oxygen atoms of 1 are highlighted.

cage $2b$ has D_3 symmetry, the interactions between the dione dimer are apparently not influenced by the cage and, other than aromatic donor–acceptor interaction with the two triazine ligands 5 , no significant interaction between the host and the guest are apparent (Figure S33, Supporting Information). Electrostatic repulsion between the dione groups is another possibility to induce the head-to-tail fashion, but the crystal structure of $2d\supset(1)_3$ (discussed next) suggested dipole–dipole interaction is more predominant.

Triple Stack ($2d\supset(1)_3$). An aromatic triple stack requires a cavity of ~ 13.2 Å (the sum of van der Waals radii: ~ 3.3 Å \times 4) and *trans*-1,2-bis(4-pyridyl)ethene pillar ($6d$) suffices to generate the appropriately sized cage $2d$. After heating an aqueous solution of dione 1 , pillar $6d$, triazine ligand 5 , and (en) $\text{Pd}(\text{NO}_3)_2$ (7) in a 3:3:2:6 ratio for 3 h at 60 °C, the formation of a single product was observed by ^1H NMR. The product was fully assigned as $2d\supset(1)_3$ by the 1D and 2D NMR analyses (Figure 4). In the ^1H NMR, two sets of guest signals, 1_{out} and 1_{in} , were observed in a 2:1 ratio (Figure 4b; see integral ratios of $H_{a-d} : H_{e-h} = 2:1$) and the host:guest signal ratio ($2d:1$) was estimated to be 1:3. The guest signals are shifted considerably upfield ($\Delta\delta = -1.13 \sim -2.96$ ppm) due to the shielding by the aromatic framework of $2d$. In a DOSY study, all the signals derived from both the host and the guests showed the same diffusion coefficient ($D = 1.4 \times 10^{-10} \text{ m}^2 \text{ s}^{-1}$).

As previously reported, the triple stacked structure of 1 was successfully determined by single-crystal X-ray analysis (Figure

(7) Aromatics with electron-withdrawing substituents are known to form very strong aromatic interactions. Most importantly, the decreased π -electron density in the aromatic ring leads to reduced π -electron repulsion. And secondly, attractive dipole–dipole interactions are increased See: Janiak, C. *Dalton Trans.* **2000**, 3885–3896.

(8) Fujita, M.; Oguro, D.; Miyazawa, M.; Oka, H.; Yamaguchi, K.; Ogura, K. *Nature* **1995**, 378, 469–471.

(9) Fujita, M.; Yazaki, J.; Ogura, K. *J. Am. Chem. Soc.* **1990**, 112, 5645–5647.

(10) (a) Beck, S.; Geyer, A.; Brintzinger, H. *Chem. Commun.* **1999**, 2477–2478. (b) Keresztes, I.; Williard, P. G. *J. Am. Chem. Soc.* **2000**, 122, 10228–10229. (c) Valentini, M.; Pregosin, P. S.; Rügger, H. *Organometallics* **2000**, 19, 2551–2555. (d) Hori, A.; Kumazawa, K.; Kusukawa, T.; Chand, K. D.; Fujita, M.; Sakamoto, S.; Yamaguchi, K. *Chem.—Eur. J.* **2001**, 7, 4142–4149.

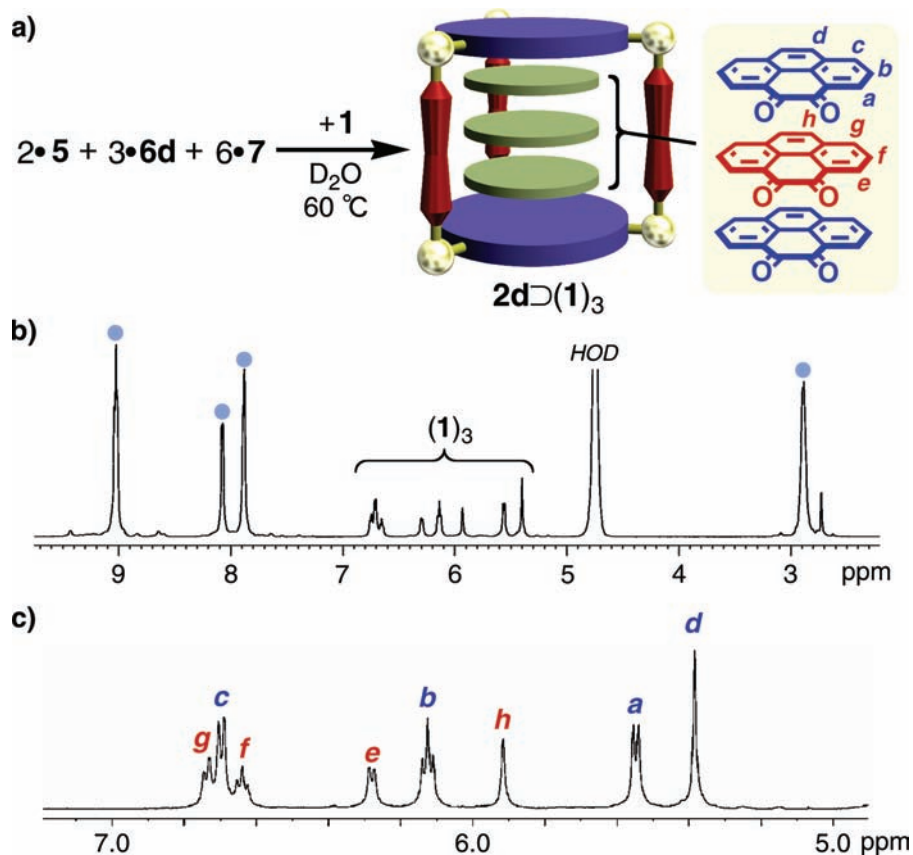


Figure 4. (a) Schematic representation of the self-assembly of triple-stacked $2d\supset(1)_3$ complex and (b) the ^1H NMR spectrum (500 MHz, 300 K) in D_2O (light blue circle: cage $2d$). (c) Magnification of $(1)_3$ region.

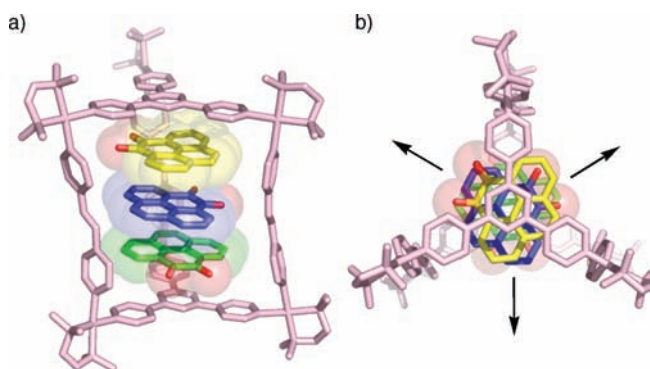


Figure 5. X-ray crystal structure of $2d'\supset(1)_3$. Hydrogen atoms, solvent molecules (H_2O) and counteranions (NO_3^-) are omitted for clarity. (a) Side view and (b) top view; carbonyl oxygen atoms of 1 are highlighted.

5 and S34, Supporting Information).¹¹ The ethylenediamine (en) *cis*-protecting groups on the Pd(II) center were first replaced with *N,N,N',N'*-tetramethylethylenediamine groups (tmed) to enhance the cage crystallinity and deep orange crystals were obtained from the slow evaporation of an aqueous solution of $2d'\supset(1)_3$ (where $2d'$ is the tmed analog of $2d$). Analysis of the structure revealed that inside cage $2d'$ the three molecules (odd number) of 1 are stacked with 3.3 \AA interplanar distances, which are shorter than that in the crystal structure of 1 itself 1 (3.54 \AA).² The shorter distance is probably due to compression by the cage's framework.^{5,11} However, the three aromatics are each

rotated 120 degrees with respect to each other, which is almost same as angular correlation among the dipoles. This orientation directly contrasts with the alternating head-to-tail stacking observed in the crystal structures of $(1)_2$ (even number) within $2b$ and free 1 . The rotated orientation cancels the net dipole moment of the host–guest structure at the expense of the local pairwise dipole–dipole interaction. As the even number of stacked molecules can align so that the local and net dipole moments are canceled, we observed an “even-odd” effect in discrete stacks of polarized 1 .

Quadruple Stack ($2e\supset(1)_4$). The crystal structures of $2b\supset(1)_2$ and $2d'\supset(1)_3$ indicate that dipole–dipole interactions are stabilizing for the formation of stacks of polarized aromatics. As this stabilization persists in the absence of crystal packing forces, larger discrete stacked structures in solution were obtained by simply extending the cage pillars. Cage $2e$ was designed to accommodate four equivalents of 1 in a quadruple stack. The calculated cavity height of 17.9 \AA should easily accommodate $(1)_4$ ($3.3 \text{ \AA} \times 5 = 16.5 \text{ \AA}$). We have been unsuccessful in obtaining any $2e\supset(G)_4$ structures with our standard, nonpolarized aromatic guests (G), typically coronene or triphenylene. The extended π -stacking of electronic-rich donor aromatic molecules is repulsive rather than attractive.⁷ However, the polarized 1 efficiently assembles in the cavity of cage $2e$ and $2e\supset(1)_4$, containing the quadruple stack $(1)_4$, is formed. When panel 5, pillar 6e, and metal hinge 7 (in a 2:3:6 ratio) were combined in D_2O with an excess amount of 1 at $60 \text{ }^\circ\text{C}$ for 3 h, we observed a very complicated ^1H NMR (Figure 6a,b). The highly upfield shifted guest signals observed at δ 4.9–6.7 ppm indicated the formation of the host–guest complex $2e\supset(1)_4$. The complex ^1H NMR spectrum is due to the presence

(11) Yamauchi, Y.; Yoshizawa, M.; Akita, M.; Fujita, M. *Proc. Natl. Acad. Sci. U.S.A.* **2009**, *106*, 10435–10437.

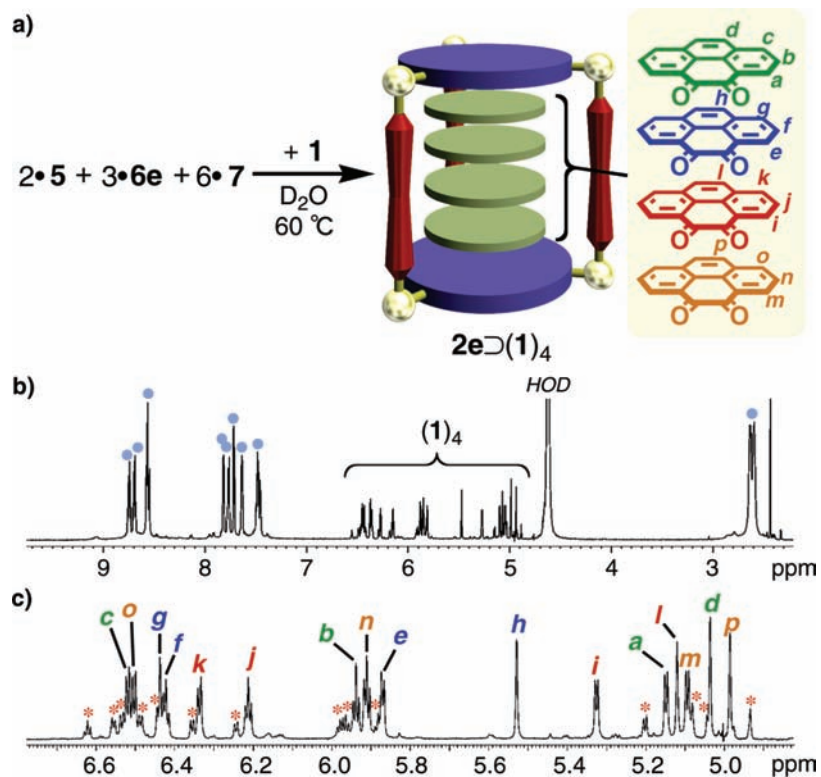


Figure 6. (a) Schematic representation of the self-assembly of quadruple-stacked $2e \supset (1)_4$ complex. (b) ^1H NMR spectra (920 MHz, 283 K) of $2e \supset (1)_4$ in D_2O (light blue circle: cage $2e$, red asterisk: 1 within cage $2e$). (c) Magnification of $(1)_4$ region.

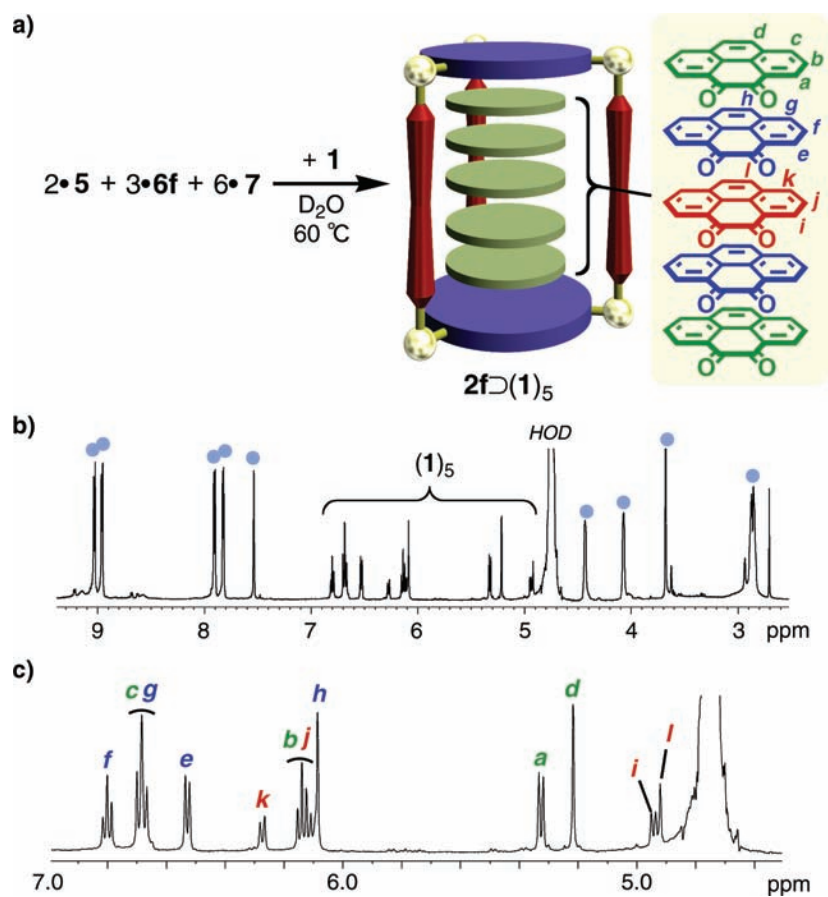


Figure 7. (a) Schematic representation of the self-assembly of quintuple-stacked $2f \supset (1)_5$ complex and (b) ^1H NMR spectrum (500 MHz, 300 K) of $2f \supset (1)_5$ in D_2O (light blue circle: cage $2f$). (c) Magnification of $(1)_5$ region.

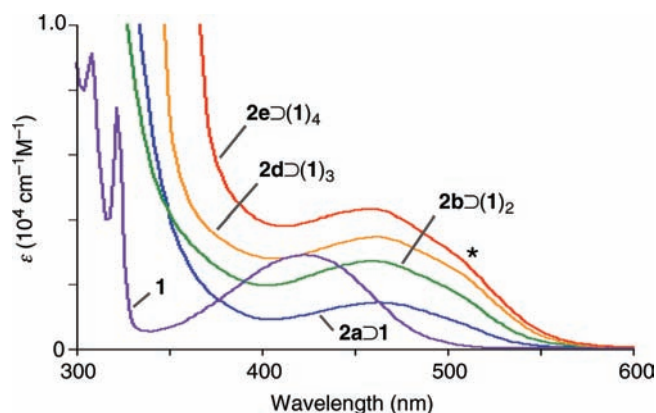


Figure 8. UV–visible spectra (RT, 1.0 mM) of $2a\supset 1$, $2b\supset(1)_2$, $2d\supset(1)_3$, and $2e\supset(1)_4$ in H_2O . **1** in CH_3CN .

of two structural isomers for **2e** ($2e_A$ and $2e_B$; Figure 1) and because the four guest molecules in the $(1)_4$ structure are nonequivalent. Careful analysis using a 920 MHz NMR spectrometer enabled the identification of the two isomers $2e_A\supset(1)_4$ and $2e_B\supset(1)_4$ (Figure 6c). The sixteen protons H_a-H_p , derived from the four nonequivalent guest molecules of the major isomer $2e_B\supset(1)_4$ were fully assigned using 2D NMR studies (Figure 6c). Signal integration revealed that isomers $2e_A\supset(1)_4$ and $2e_B\supset(1)_4$ are formed in a statistical 1:3 ratio.

Quintuple Stack ($2f\supset(1)_5$). Further elongation of the pillar ligand led to the formation of the quintuple stacks of dione **1**. We employed 1,4-di(4-pyridylethynyl)-2,5-di(2-methoxyethoxy)-benzene (**6f**) as the pillar for quintuple aromatic stacks. The two methoxyethoxy groups are attached to the pillar to enhance the water-solubility of the cage. The self-assembly of $2f\supset(1)_5$ smoothly took place after heating a D_2O solution of panel **5**, pillar **6f**, and metal hinge **7** in the presence of excess **1** at 60 °C for 3 h (Figure 7a). The selective formation of cage **2f** containing five molecules of **1** was clearly shown by 1H NMR by the following observations: (i) the integral ratio of cage **2f** and **1** was estimated to 1:5 and (ii) three sets of proton signals derived from $(1)_5$ are present in a 2:2:1 ratio ($H_{a-d}: H_{e-h}: H_{i-l} = 2:2:1$) (Figure 7b,c). Detailed 2D NMR analyses also supported the formation of a quintuple stacking structure.

Absorption Spectra. UV–vis absorption spectra were measured for the series of $2\supset(1)_n$ ($n = 1-5$) inclusion complexes (Figure 8). For the single stack ($n = 1$) the Pt(II) cage **2a** was employed as the Pd(II) cage is in equilibrium with the homotopic complexes. The $n-\pi^*$ transition of **1** in CH_3CN is a broad absorption at $\lambda_{max} = 422$ nm ($\epsilon = 2.9 \times 10^3$ $cm^{-1} M^{-1}$). In $2a\supset 1$, this absorption band is significantly red-shifted ($\lambda_{max} = 462$; $\Delta\lambda = 40$ nm) due to aromatic interactions with triazine panel **5** of **2a**. Similar absorptions were observed for the series of $2\supset(1)_n$ ($n = 3, 4$) and the stepwise of accumulation of **1** in the $2\supset(1)_n$ structures ($n = 2-5$) in solution is apparent. In the solid state, the spectrum of **1** shows a broad absorption at $\lambda_{max} = 525$, which is attributed to intermolecular aromatic interactions in the infinite columnar stack of alternating **1**. A similar broad absorption appears as a shoulder ($\lambda_{max} = 510$ nm; $\epsilon = 1.5 \times 10^3$ $cm^{-1} M^{-1}$) in the solution-state spectra of discrete stacks $2b\supset(1)_n$, where $n = 2$, and indicates similar intermolecular aromatic interactions as in the solid state.

Conclusion

We confirmed that the dipole–dipole interactions as well as π -stacking interactions of a polarized aromatic molecule suffice

to form columnar aromatic stacks in the absence of crystal packing forces, even in the solution state. In addition, we showed that discrete, double and triple stacks of polarized molecules can display unique stacking orientations in the crystalline state. In even numbered stacks, the molecules align in a head to tail fashion so that the local and net dipoles cancel. In odd numbered stacks, the molecules adopt an orientation where the net dipole is canceled at the expense of the local dipole interactions. The stabilizing dipole interactions enable the formation of extended, discrete aromatic stacks through intermolecular π -stacking interactions. Pillared cages **2a–2f** enable the precise control of the stacking number without restricting the orientation of the guests, providing opportunities to study the hitherto unexplored properties of discrete stacks of aromatic compounds in solution.¹²

Experimental Section

Preparation of $2a\supset 1$. Powder of **1** (4.6 mg; 20 μ mol, 2 equiv per **2a**) was added to a D_2O solution (1.0 mL) of cage **2a** (31.0 mg; 10 μ mol) and the suspended mixture was stirred at 60 °C for 30 min. After filtration of the resulted orange solution, the 1H NMR spectrum revealed the quantitative formation of $2a\supset 1$ complex. The resulting solution was dried by a freeze-drying equipment to give $2a\supset 1$ as an orange powder (31 mg, 92% yield). 1H NMR (500 MHz, D_2O , 300 K, TMS as an external standard): δ 9.59 (s, 12H), 9.08 (d, $J = 5.5$ Hz, 12H), 8.14 (br, 12H), 7.53 (d, $J = 7.5$ Hz, 2H), 7.86 (t, $J = 7.5$ Hz, 2H), 6.30 (s, 2H), 6.20 (d, $J = 7.5$ Hz, 2H), 2.89 (d, $J = 5.5$ Hz, 12H), 2.84 (d, $J = 5.5$ Hz, 12H); ^{13}C NMR (125 MHz, D_2O , 300 K): δ 177.9 (C_q), 167.8 (C_q), 153.5 (CH), 151.3 (CH), 144.3 (C_q), 135.9 (CH), 131.1 (CH), 130.1 (C_q), 128.9 (CH), 127.8 (C_q), 127.4 (CH), 125.6 (CH), 47.7 (CH₂); DOSY (m^2/s): $\log D = -9.80$; IR (KBr, cm^{-1}): 3420(br), 3040(br), 1512, 1383, 823, 816, 722, 705; m.p.: ~ 230 °C (decomposed).

Preparation of $2b\supset(1)_2$. A mixture of pillar ligand **6b** (6.4 mg, 30 μ mol), panel ligand **5** (6.3 mg, 20 μ mol), (en)Pd(NO₃)₂ (**7**; 17.4 mg, 60 μ mol), and pyrene-4,5-dione (**1**; 5.0 mg, 22 μ mol) in D_2O (1.0 mL) was stirred at 100 °C for 3 h to give clear orange solution. 1H NMR analysis of the solution revealed the formation of $2b\supset(1)_2$. After filtration of the resulted orange solution, the resulting solution was dried by a freeze-drying equipment. $2b\supset(1)_2$ was isolated as an orange powder (31 mg, 91% yield). 1H NMR (500 MHz, D_2O , 300 K, TMS as an external standard): δ 8.79 (d, $J = 4.5$ Hz, 12H), 7.99 (s, 12H), 7.94 (d, $J = 4.5$ Hz, 12H), 6.66 (br, 4H), 6.03 (br, 8H), 5.84 (s, 4H), 3.69 (s, 36H), 2.99 (d, $J = 5.3$ Hz, 12H), 2.92 (d, $J = 5.3$ Hz, 12H); ^{13}C NMR (125 MHz, D_2O , 300 K): δ 177.8 (C_q), 168.0 (C_q), 161.2 (CH), 152.5 (CH), 148.0 (C_q), 143.8 (C_q), 136.1 (CH), 129.9 (C_q), 128.6 (CH), 127.3 (CH), 126.6 (C_q), 126.2 (CH), 125.0 (C_q), 124.8 (CH), 122.8 (CH), 47.6 (CH₂), 46.5 (CH₂), 25.9 (CH₃); DOSY (m^2/s): $\log D = -9.83$; IR (KBr, cm^{-1}): 3407(br), 3067(br), 2391(br), 2285(br), 1670, 1617, 1576, 1519, 1384, 1359, 1273, 1053; m.p.: ~ 230 °C (decomposed); E.A. Calcd for C₁₂₂H₁₃₆N₄₂O₄₀Pd₆•27(H₂O): C, 37.04; H, 4.84; N, 14.87. Found: C, 36.78; H, 4.60; N, 14.75; X-ray crystal data of $2b\supset(1)_2$: C_{122.5}H₁₂₀N_{35.5}O₄₅Pd₆, $M_r = 3447.91$, crystal dimensions 0.15 \times 0.12 \times 0.05 mm³, monoclinic space group $P2_1/c$, $a = 19.336(20)$ Å, $b = 37.32(3)$ Å, $c = 27.17(3)$ Å, $\beta = 100.48(4)^\circ$, $V = 19278(32)$ Å³, $Z = 4$, $\rho_{calcd} = 1.188$ g cm⁻³, $F(000) = 6958$, radiation, λ (Mo

- (12) (a) Yoshizawa, M.; Ono, K.; Kumazawa, K.; Kato, T.; Fujita, M. *J. Am. Chem. Soc.* **2005**, *127*, 10800–10801. (b) Yoshizawa, M.; Kumazawa, K.; Fujita, M. *J. Am. Chem. Soc.* **2005**, *127*, 13456–13457. (c) Ono, K.; Yoshizawa, M.; Kato, T.; Watanabe, K.; Fujita, M. *Angew. Chem., Int. Ed.* **2007**, *46*, 1803–1806. (d) Ono, K.; Yoshizawa, M.; Kato, T.; Fujita, M. *Chem. Commun.* **2008**, 2328–2330. (e) Yamauchi, Y.; Yoshizawa, M.; Fujita, M. *J. Am. Chem. Soc.* **2008**, *130*, 5832–5833. (f) Ono, K.; Yoshizawa, M.; Akita, M.; Kato, T.; Tsunobuchi, Y.; Ohkoshi, S.; Fujita, M. *J. Am. Chem. Soc.* **2009**, *131*, 2782–2783. (g) Sawada, T.; Yoshizawa, M.; Sato, S.; Fujita, M. *Nat. Chem.* **2009**, *1*, 53–56.

$K\alpha$) = 0.71073 Å, $T = 90(2)$ K, reflections collected/unique 145498/47851 ($R_{\text{int}} = 0.2351$). The structure was solved by direct methods (SHELXL-97) and refined by full-matrix least-squares methods on F^2 with 1515 parameters. $R_1 = 0.1887$ ($I > 2\sigma(I)$), $wR_2 = 0.5792$, GOF 1.066; max/min residual density 3.317/−2.340 $\text{e}\text{\AA}^{-3}$. CCDC reference number 732820.

Preparation of 2d(1)3. A mixture of pillar ligand **6d** (5.5 mg, 30 μmol), panel ligand **5** (6.3 mg, 20 μmol), (en)Pd(NO₃)₂ (**7**; 17.4 mg, 60 μmol), and pyrene-4,5-dione (**1**; 7.0 mg, 30 μmol) in D₂O (1.0 mL) was stirred at 60 °C for 3 h to give clear orange solution. ¹H NMR analysis of the solution revealed the formation of **2d(1)3** quantitatively. After filtration of the resulted orange solution, the resulting solution was dried by a freeze-drying equipment. **2d(1)3** was isolated as an orange powder (33 mg, 91% yield). ¹H NMR (500 MHz, D₂O, 300 K, TMS as an external standard): δ 9.02 (d, $J = 6.5$ Hz, 12H), 9.01 (d, $J = 6.5$ Hz, 12H), 8.06 (d, $J = 6.5$ Hz, 12H), 7.87 (d, $J = 6.5$ Hz, 12H), 7.86 (s, 6H), 6.74 (d, $J = 7.5$ Hz, 2H), 6.70 (d, $J = 7.5$ Hz, 4H), 6.64 (d, $J = 6.5$ Hz, 2H), 6.28 (d, $J = 6.5$ Hz, 2H), 6.13 (t, $J = 7.5$ Hz, 4H), 5.92 (s, 2H), 5.55 (d, $J = 7.0$ Hz, 4H), 5.39 (s, 4H), 2.87 (br, 24H); ¹³C NMR (125 MHz, D₂O, 300 K): δ 177.2 (C_q), 176.6 (C_q), 167.9 (C_q), 152.2 (CH), 151.7 (CH), 147.5 (C_q), 143.6 (C_q), 136.4 (CH), 136.0 (CH), 132.4 (CH), 129.6 (C_q), 129.3 (C_q), 128.7 (CH), 128.7 (CH), 127.7 (CH), 127.2 (CH), 126.0 (C_q), 126.0 (CH), 125.7 (CH), 124.7 (CH), 124.7 (CH), 124.6 (C_q), 46.8 (CH₂); DOSY (m²/s): log $D = -9.85$; IR (KBr, cm⁻¹): 3410(br), 3200(br), 3080(br), 1670, 1614, 1519, 1383, 1061, 831, 804; m.p.: ~230 °C (decomposed); E.A. Calcd. for C₁₃₂H₁₂₆N₄₂O₄₂Pd₆•20(H₂O): C, 39.92; H, 4.21; N, 14.81. Found: C, 39.76; H, 4.02; N, 15.00; X-ray crystal data of **2d'(1)3**: C₁₅₆H₁₇₄N₃₈O_{65.5}Pd₆, $M_r = 4259.74$, crystal dimensions 0.15 × 0.15 × 0.05 mm³, monoclinic space group $P2_1/c$, $a = 28.563(4)$ Å, $b = 16.085(2)$ Å, $c = 41.635(5)$ Å, $\beta = 94.598(3)^\circ$, $V = 19067(4)$ Å³, $Z = 4$, $\rho_{\text{calcd}} = 1.487$ g cm⁻³, $F(000) = 8704$, radiation, $\lambda(\text{Mo K}\alpha) = 0.71073$ Å, $T = 80(2)$ K, reflections collected/unique 141967/47437 ($R_{\text{int}} = 0.1607$). The structure was solved by direct methods (SHELXL-97) and refined by full-matrix least-squares methods on F^2 with 2584 parameters. $R_1 = 0.1246$ ($I > 2\sigma(I)$), $wR_2 = 0.4073$, GOF 0.966; max/min residual density 4.611/−1.703 $\text{e}\text{\AA}^{-3}$. CCDC reference number 703950.

Preparation of 2e(1)4. A mixture of pillar ligand **6e** (3.8 mg, 15 μmol), panel ligand **5** (3.2 mg, 10 μmol), (en)Pd(NO₃)₂ (**7**; 8.7 mg, 30 μmol), and pyrene-4,5-dione (**1**; 4.6 mg, 20 μmol) in D₂O (1.0 mL) was stirred at 60 °C for 3 h to give a clear orange solution. ¹H NMR analysis of the solution revealed the formation of **2e(1)4**. After filtration of the resulted orange solution, the resulting solution was dried by a freeze-drying equipment. **2e(1)4** was isolated as an orange powder (18 mg, 87% yield). ¹H NMR (920 MHz, D₂O, 283 K, TMS as an external standard): δ 8.83 (m, 6H), 8.79 (m, 6H), 8.66 (m, 12H), 7.90 (d, $J = 6.4$ Hz, 6H), 7.86 (d, $J = 6.4$ Hz, 6H), 7.80 (d, $J = 6.4$ Hz, 6H), 7.72 (d, $J = 6.4$ Hz, 6H), 7.55 (m, 12H), 6.52 (d, $J = 7.4$ Hz, 2H), 6.50 (d, $J = 7.4$ Hz, 2H), 6.44 (d, $J = 7.4$ Hz, 2H), 6.42 (t, $J = 7.4$ Hz, 2H), 6.34 (d, $J = 7.4$ Hz, 2H),

6.21 (d, $J = 7.4$ Hz, 2H), 5.94 (t, $J = 7.4$ Hz, 2H), 5.91 (t, $J = 7.4$ Hz, 2H), 5.87 (d, $J = 7.4$ Hz, 2H), 5.53 (s, 2H), 5.32 (d, $J = 7.4$ Hz, 2H), 5.15 (d, $J = 7.4$ Hz, 2H), 5.12 (s, 2H), 5.09 (d, $J = 7.4$ Hz, 2H), 5.03 (s, 2H), 4.98 (s, 2H), 2.64 (br, 12H), 2.61 (br, 12H); ¹³C NMR (125 MHz, D₂O, 300 K): δ 177.0 (C_q), 176.2 (C_q), 167.7 (C_q), 152.0 (CH), 151.7 (CH), 151.3 (CH), 143.5 (C_q), 137.0–135.5 (m), 133.7 (CH), 129.4–127.2 (m), 125.8–124.5 (m), 98.0 (C_q), 87.1 (C_q), 46.7 (CH₂); DOSY (m²/s): log $D = -9.88$; IR (KBr, cm⁻¹): 3418(br), 3205(br), 3080(br), 1672, 1618, 1523, 1384, 1360, 1064, 889; m.p.: ~230 °C (decomposed); E.A. Calcd. for C₁₆₆H₁₄₀N₄₂O₄₄Pd₆•26(H₂O): C, 43.97; H, 4.27; N, 12.97. Found: C, 43.67; H, 3.92; N, 13.17.

Preparation of 2f(1)5. A mixture of pillar ligand **6f** (7.9 mg, 18 μmol), panel ligand **5** (3.1 mg, 10 μmol), (en)Pd(NO₃)₂ (**7**; 8.7 mg, 30 μmol), and pyrene-4,5-dione (**1**; 6.5 mg, 27 μmol) in D₂O (1.0 mL) was stirred at 60 °C for 3 h to give clear orange solution. ¹H NMR analysis of the solution revealed the formation of **2f(1)5**. After filtration of the resulted orange solution, the resulting solution was dried by a freeze-drying equipment. **2f(1)5** was isolated as an orange powder (21 mg, 85% yield). ¹H NMR (500 MHz, D₂O, 300 K, TMS as an external standard): δ 9.03 (d, $J = 6.0$ Hz, 12H), 8.96 (d, $J = 5.3$ Hz, 12H), 7.91 (d, $J = 6.0$ Hz, 12H), 7.82 (d, $J = 5.3$ Hz, 12H), 7.54 (s, 6H), 6.80 (t, $J = 7.5$ Hz, 4H), 6.70–6.67 (m, 8H), 6.53 (d, $J = 7.0$ Hz, 4H), 6.27 (d, $J = 7.5$ Hz, 2H), 6.16–6.11 (m, 6H), 6.09 (s, 4H), 5.22 (d, $J = 7.0$ Hz, 4H), 5.22 (s, 4H), 4.94 (d, $J = 7.5$ Hz, 2H), 4.92 (s, 2H), 4.43 (br, 12H), 4.07 (br, 12H), 3.68 (s, 18H), 2.87 (br, 12H) 2.85 (br, 12H); ¹³C NMR (125 MHz, D₂O, 300 K): δ 177.0 (C_q), 176.3 (C_q), 175.7 (C_q), 167.8 (C_q), 154.3 (CH), 152.1 (CH), 151.4 (CH), 143.6 (C_q), 136.2 (CH), 135.8 (CH), 135.5 (C_q), 135.0 (CH), 129.4 (C_q), 129.3 (CH), 129.0 (C_q), 128.7 (CH), 128.7 (CH), 128.5 (CH), 128.3 (C_q), 127.6 (CH), 127.2 (CH), 126.7 (CH), 126.0 (CH), 126.0 (C_q), 125.9 (CH), 125.8 (C_q), 125.7 (C_q), 125.4 (CH), 124.7 (CH), 124.6 (C_q), 124.4 (C_q), 124.2 (C_q), 118.3 (C_q), 114.0 (C_q), 94.7 (C_q), 91.9 (C_q), 70.9 (CH₂), 69.4 (CH₂), 58.9 (CH₃), 46.8 (CH₂); DOSY (m²/s): log $D = -9.90$; IR (KBr, cm⁻¹): 3439(br), 3200(br), 3077(br), 2205(br), 1667, 1610, 1522, 1384, 1375, 1221, 1127, 1061; m.p.: ~230 °C (decomposed).

Acknowledgment. We thank Prof. K. Kato, M. Nakano of Institute for Molecular Science and Prof. Y. Yamaguchi of RIKEN for help with 920 MHz NMR measurements. Y.Y. thanks for a JSPS Research Fellowship for Young Scientists. This research was supported in part by Global COE Program (Chemistry Innovation through Cooperation of Science and Engineering), MEXT, Japan.

Supporting Information Available: Experimental details and spectroscopic data. This material is available free of charge via the Internet at <http://pubs.acs.org>.

JA904063R